

Effect of daily setup errors on individual dose distribution in conventional radiotherapy: An initial study

メタデータ	言語: eng 出版者: 公開日: 2017-10-03 キーワード (Ja): キーワード (En): 作成者: メールアドレス: 所属:
URL	http://hdl.handle.net/2297/19140

Title

Effect of daily setup errors on the individual dose distribution in conventional radiotherapy – an initial study –

Names

Akihiro Takemura, Saori Shoji*, Sinichi Ueda*, Yuichi Kurata*, Tomoyasu Kumano**, Shigeyuki Takamatsu**, Masayuki Suzuki

Division of Health Sciences, Graduate School of Medical Science, Kanazawa University
5-11-80 Kodatsuno, Kanazawa 920-0942 Japan

*Kanazawa University Hospital

1-13 Takaramachi, Kanazawa 920-8641 Japan

**Department of Radiology, Graduate School of Medical Science, Kanazawa University
1-13 Takaramachi, Kanazawa 920-8641 Japan

Concise and informative title

Effect of daily setup errors on the individual dose distribution

Corresponding author

Akihiro Takemura

Email: at@mhs.mp.kanazawa-u.ac.jp Telephone: +81-76-265-2538

Fax: +81-76-234-4366

Abstract

Recent linear accelerators can perform cone beam computed tomography to correct setup errors immediately before dose delivery. We calculated the dose distribution with setup errors acquired from cone beam computed tomography to determine more realistic and individual effect of the setup errors. The differences in dose distribution were analyzed. The setup errors of three patients who were irradiated in the neck, esophagus and pelvic area were obtained retrospectively. We found that the maximum dose variances for the three cases were 19.9 to 35.9%. The maximum dose variance points were relatively far from the isocenter. The volume of the 10% dose difference had widths of 1.3 to 1.85 cm around the beam edges. The V95 and mean doses at the clinical target volume were mostly unchanged. Doses around the beam edges were more varied than those around the isocenter for every case. The dose on the spinal cord located near the beam edges varied by 5 – 10 % compared with the dose of the radiotherapy plan in two of the cases. We demonstrated the individual dose distributions of the cases affected by daily setup errors for all fractions.

Keywords

Radiotherapy, Setup error, Dose distribution, Image-guided radiotherapy, Cone-beam CT

Introduction

Setup errors at each fraction of radiotherapy can cause dose variation in a patient's body, and thus may deliver an unexpected under-dose to a tumor and/or overdose to normal tissue. The American Association of Physicists in Medicine Report 13 [1] states that the spatial uncertainty of external radiotherapy should be smaller than 10 mm and also that the error of patient setup included in the spatial uncertainty should be smaller than 6 mm. More highly accurate patient localization is currently required in stereotactic irradiation. Methods for measuring setup errors have been developed, and registration methods have been developed for correction of setup errors.

In previous studies, setup errors were measured in patients who were irradiated in the whole pelvic area by using a portal image and a digitally reconstructed radiograph (DRR) reconstructed from computed tomography (CT) images [2] and in patients whose livers were irradiated with stereotactic body radiation therapy [3]. Kunzler et al, [4] developed a registration method for a DRR and a portal image of stereotactic irradiation. Several authors have reported their two dimensional (2D) – three dimensional (3D) registration methods of volume data from CT or cone-beam CT (CBCT) and a portal image [5-8]. Lerourneau et al [9] measured setup errors by using 3D-3D registration of CT volume data and CBCT volume data.

There have been several studies that have estimated the effects of setup errors on dose distribution. Wang et al. [10] described the effect of setup errors in stereotactic body radiotherapy of spinal metastasis obtained by a simulation. Intensity modulated radiation therapy (IMRT) for head and neck tumors has also been described [11, 12]. However, the

results from these studies were obtained from simulations, e.g., estimated values of errors and variance were used and actual setup errors were not used.

The effects of actual setup errors have been calculated in three separate studies. Two of these studies [13,14] obtained setup error data by using portal images or radiographs with the on-board imaging system. These images were 2D images, and thus only translational setup error was taken into account in the studies. Rotational error is an alternative component of setup error. The other study [15] used CT images performed frequently during the treatment course. However, the CT sessions were performed up to 15 times in 77 fractions per case. Another study [16] obtained setup errors by using CT images and a portal image to develop their mathematical model, and then calculated the difference in the biological effective dose (BED). The effect of random error in the patient setup on the BED has been calculated previously [17].

Many studies have focused on obtaining the general effect of setup errors to determine sufficient planning target volume (PTV) margin. We believe that it is important to clarify an individual dose distribution affected by daily setup errors for all fractions, and these dose distributions could make it possible to assess treatment dose including effects of setup errors.

Therefore, we selected three cases irradiated in the chest, head and neck, and pelvic area, and analyzed the differences in the dose distribution. In this study, we obtained 3D daily setup errors of all fractions in a radiotherapy plan obtained by using a 3D-3D registration of CT volume data and CBCT volume data acquired immediately before irradiation to determine a more realistic assessment of dose variation due to setup errors.

Materials and Methods

We used a linear accelerator (Linac) integrated with an X-ray and flat panel detector (FPD) system (Elekta Synergy, Elekta AB, Stockholm, Sweden). The X-ray and FPD system was mounted on the gantry system of the Linac, and the beam direction of the Linac and that of the X-ray and FPD system were orthogonal to each other.

The X-ray and FPD system can perform CBCT and can provide 3D volume data on a patient just before irradiation. In general, the CBCT volume data are immediately registered with CT volume data for radiotherapy planning for calculation of errors in patient positioning. The couch is then moved to correct these errors.

Using this system, we obtained setup errors, which consisted of translational errors for a patient in the X, Y and Z directions and rotational errors for a patient around each axis. Systematic components (mean) and random components (standard deviation) of the setup errors for each axis and each case are shown in Table 1. The X axis indicates the lateral direction (right to left) of a patient, the Y axis indicates the longitudinal direction (inferior to superior) and the Z axis indicates the vertical direction (posterior to anterior) (Fig. 1). CBCT and registration were performed routinely at every dose fraction for many cases in the hospital, and thus setup error data were obtained retrospectively. A small field of view (270 mm in diameter in the XY plane and 264 mm in the Z axis; a 512 x 512 x 512 matrix) was used for all acquisitions. The algorithm of registration was bone matching, which used the bone structure of the patient to calculate positional errors.

We developed a radiotherapy plan with setup errors to obtain dose distribution

affected by daily setup errors. This plan was built from the approved plan, which was used for the actual treatment. All beams in the approved plan were copied for every fraction; for example, the approved plan had four beams and 20 fractions, and therefore, a plan with 80 beams was designed. Alignment of all beams was rearranged for producing the daily setup errors. The beam alignment was calculated by transformation between the orthogonal coordinate system and the sphere coordinate system, and by affine transformation. The gantry angle and couch angle are components in a sphere coordinate system that originates at the isocenter; the tilt angle stands for the gantry angle and the azimuth angle stands for the couch angle. Setup errors are the components in an orthogonal coordinate system.

To produce setup errors, the source position in the orthogonal coordinate system should be determined first. Thus the source position represented by the gantry angle, couch angle and source-isocenter distance should be transferred to orthogonal coordinates. That is defined as follows;

$$S \begin{pmatrix} x \\ y \\ z \end{pmatrix} = \begin{pmatrix} r \sin \theta \cos \phi \\ r \sin \theta \sin \phi \\ r \cos \theta \end{pmatrix} \text{----- (1)}$$

Where, θ is the tilt (gantry) angle, ϕ is the azimuth (couch) angle, and r is the source-isocenter distance. The source position in the orthogonal coordinate system is transformed by the affine transformation with rotational setup errors. The affine transformation was calculated as follows:

$$P \begin{pmatrix} x' \\ y' \\ z' \end{pmatrix} = T \times S \begin{pmatrix} x \\ y \\ z \end{pmatrix} \text{----- (2)}$$

Where, T is a transfer matrix. In the case of a coordinate system as shown in Fig. 1, it's defined as follows:

$$T = \begin{pmatrix} 1 & 0 & 0 \\ 0 & -\cos R_x & \sin R_x \\ 0 & -\sin R_x & -\cos R_x \end{pmatrix} \begin{pmatrix} \cos R_y & 0 & \sin R_y \\ 0 & 1 & 0 \\ -\sin R_y & 0 & \cos R_y \end{pmatrix} \begin{pmatrix} -\cos R_z & \sin R_z & 0 \\ -\sin R_z & -\cos R_z & 0 \\ 0 & 0 & 1 \end{pmatrix} \dots\dots\dots (3)$$

Where, R_x , R_y , and R_z are the rotational errors of X, Y and Z axes at a fraction, respectively.

P is a source position producing rotational setup errors. $P(x',y',z')$ in the orthogonal coordinate system is transferred to the coordinates in the sphere coordinate system as follows:

$$\theta' = \tan^{-1} \left(\frac{z'}{\sqrt{x'^2 + y'^2}} \right) \dots\dots\dots(4)$$

$$\phi' = \tan^{-1} \left(\frac{y'}{x'} \right) \dots\dots\dots(5)$$

The translational errors were represented by shifting the isocenter.

A radiotherapy planning system (RTPS), Xio Release 4.3.1 (CMS Inc., St. Louis, Missouri, USA), was used for making the radiotherapy plan. The dose calculation algorithm was the superposition method. However, the RTPS has a constraint on the number of beams; 99 beams is the maximum. Therefore, we had to select cases, which had a smaller product of the number of beams and the number of fractions than the limitation of the number of beams.

In this study, we retrospectively obtained three cases who were irradiated in the neck, esophagus, and coccygeal bone area (a 62 year-old man, a 74 year-old man and a 50 year-old woman, respectively) as initial cases. We chose one patient for each irradiated site

in the head-and-neck, chest, and abdomen or pelvic area for the initial cases. Additionally, patients with lung or abdominal tumors were not selected to eliminate the effect of respiratory motion. Whole pelvic irradiation is not performed using the Linac because of the maximum field size of the multileaf collimator. The maximum field size (21 cm x 16 cm) is not large enough to cover the area for whole pelvic irradiation. Another Linac at our institution is able to perform whole pelvic irradiation, but CBCT is not performed at every fraction.

We obtained CBCT registration results as setup error data from the three patients. The patients treated in the neck, esophagus and coccygeal bone were called cases A, B, and C, respectively. Case A was irradiated by oblique parallel opposing fields (1st port 315 degrees, 2nd port 135 degrees) with 15 degree wedges and was immovable with a head and neck shell (ESS-24, Engineering System Co. Ltd., Japan). The number of fractions was 30 and the total dose was 6000 cGy (6MV X-ray). Case B was irradiated by oblique parallel opposing fields (1st port 320 degrees, 2nd port 140 degrees) without wedges and used an arm support pillow (ESF-18, Engineering System Co. Ltd., Japan). The number of fractions was 10 and the total dose was 2000 cGy (10MV X-ray). Case C was irradiated by cross-fire fields (1st port 0 degrees, 2nd port 90 degrees, 3rd port 180 degrees, 4th port 270 degrees) and the 3rd and 4th ports had a 20 degree wedge filter added and a heel support pillow (ESS-38, Engineering System Co. Ltd., Japan) was used. The number of fractions was 20 and the total dose was 6000 cGy (10MV X-ray). Elekta Synergy has a motorized (internal physical) wedge system, and thus the wedge angle is flexible

The beam isocenter was placed at the center of the clinical target volume (CTV),

which was delineated by the radiation oncologists. The dose was normalized by the dose at the isocenter. The multi-leaf collimator (MLC) leaf position is usually determined by the volume, which is the CTV plus the PTV margin of 5 mm and MLC margin of 5 mm (total 10 mm); however, the MLC leaf position is sometimes edited according to the case. In the radiotherapy plan for case C, the MLC margin was extended up to 10 mm. For cases A and B, only CTV was delineated and the MLC leaf position was determined by adding a 10 mm margin (5 mm PTV margin + 5 mm MLC margin) to the CTV. A summary of the three cases is shown in Table 1 and the beam alignment of their approved plans is shown in Fig. 2.

We calculated the dose distribution of the plan with setup errors and then subtracted the dose distribution of the approved plan to determine the difference between these dose distributions. In the differential dose distribution, the maximum width of the iso-dose volume of the 10% dose and the maximum dose difference were measured. The dose expressed as a percentage in the differential dose distribution was based on the total dose (i.e., 6000 cGy for cases A and C and 2000 cGy for case B). The width of the iso-dose volume of the 10% dose was orthogonal to the beam direction. The width was measured at several depths along each beam and the maximum width was obtained. The maximum dose difference is the maximum variation between the dose distributions of the approved plan and the plan with setup errors.

Dose-volume histograms (DVHs) of the CTV and organs at risk (ORs) of the plans with the setup errors were compared with those of the approved plans, and V95, the volume covered by 95% or more of the dose, and the mean dose of the CTV for each case was

calculated.

Results

Figure 3 shows the dose distributions of the approved plans, the plans with setup errors and the subtractions of these dose distributions in each case. These particular slices were chosen because they showed a relatively large dose variation. The dose distributions for the approved plan and the plan with setup errors are similar to each other, but in the differential dose distribution, the dose was varied. The differential dose distribution showed that the dose variation appeared along the beam edges. Additionally, a region of 5 – 10% dose difference overlapped a part of the spinal cord of cases A and B.

The maximum dose differences were 34.7% for case A, 35.9% for case B and 19.9% for case C. The maximum dose difference point was located on the beam edge and relatively far from the isocenter.

The maximum widths of the iso-dose volume of the 10% dose difference were 1.7 cm for case A, 1.6 cm for case B and 1.3 cm for case C.

The DVHs for the CTV in the plan with setup errors for all cases were similar to those of the approved plan and the DVH for the PTV in the plan with setup errors for case C was slightly decreased from that of the approved plan (Fig. 4). Results of V95 and mean dose are shown in Table 2. The differences of V95s of CTV between the approved plan and the plan with setup errors were 1.9% for case A, 0.4% for case B and 0.1% for case C (7.8% for the PTV of case C) The differences in mean doses of the CTVs between the approved plan and the plan with setup errors were 0.5% for case A, 0.3% for case B and

0.4% for case C (0.8% of PTV). No major differences were found in the V95 and mean dose between the plans. The DVH for the spinal cord in the plan with setup errors of case B, which was located near the CTV, was slightly increased from that in the approved plan because of dose variation around the beam edges.

The maximum dose points in the differential dose distributions, where the dose was the most varied, were located along the beam edge and far from the isocenter (Fig. 5).

Discussion

We found that the dose for the CTV was not greatly affected by the setup error. The reasons for this finding are as follows: the rotational error of the setup error should change the dose in parts of the body that are located far from the isocenter more than doses around the isocenter (i. e., the CTV was located around the isocenter) and the translational error affected the dose of the beam edges because the dose intensity in the fields was uniform. If the analysis of this study is applied to dose distribution for the IMRT plan, the dose for a target may be changed.

V95 of the CTV for case C was higher than that for the other cases, and the difference between the V95s for the approved plan and for the plan with setup errors was small. The reason why there was a high V95 in case C is that case C had a wider MLC margin applied than in the other cases. However, V95 of the PTV for case C was decreased by approximately 8% in the plan with setup errors compared with the approved plan. We believe that a small PTV volume caused the decrease of V95. If the dose-modified volume in a PTV is small and a PTV is large enough, V95 should not change much. On the other

hand, if a PTV is small, V95 could change by a large amount. Case C had a small PTV (less than one fourth of the CTV for case A), and thus the V95 of PTV for case C could have been more sensitive than that for the other cases. However, differences in the mean dose and V95 of CTV between the approved plan and the plan with setup errors were small, and thus the dose to the CTV was not affected much by setup errors.

The major factor for the dose variation far from the isocenter could be due to rotational errors, and the position at the maximum dose difference was far from the isocenter. This suggests that an OR far from an isocenter and near to the beam edge could have an unexpected high dose delivered (approximately a 35% dose in this study) due to setup errors in traditional radiotherapy (without an image guided system).

On the other hand, translational errors could vary the dose around a target. The dose of an OR near a target can vary by 5 - 10% compared with a dose in the approved plan (e.g., cases A and B). Fortunately, part of the spinal cord of case A was covered by a -5% iso-dose line. However, the spinal cord might have had a higher dose delivered according to setup errors. When the plan is changed to avoid going over the tolerance dose of the OR, the volume of the OR plus a sufficient margin (i.e., planning organ at risk volume) should be defined to avoid an overdose. We found that the 10% dose region in the difference distributions had a 1.3 to 1.85 cm width around the beam edges.

The dose distribution difference probably depends upon the magnitude of the systematic setup errors. However, this is not clearly illustrated in our results. Case B had a maximum magnitude of rotational error among the three cases (i.e., a rotational error of 2.32 degrees for the X axis) and case A had the next highest value. This order of magnitude

of rotational error is equal to the order of magnitude of the maximum dose in the difference distributions. However, the order of magnitude of the translational error did not match the order of magnitude of the rotational error. The magnitude of the setup errors in this study was the same level as that reported in previous studies [1-3,5,9,11,13]. Thus we believe that the feature of dose distribution difference is caused by the setup errors for radiotherapy of each site. However, index values, such as V95 and mean dose, may be affected by volume and location of a tumor and irradiation technique. To clarify the effect of the magnitude of setup errors, we will need to analyze more cases in future studies. In addition, internal organ motion and non-rigid deformation of the body was not taken into account for in this study because they could not be measured by the Linac system. However, motion and deformation could possibly greatly affect dose distributions, and thus need to be considered in future studies.

In our hospital, a bone matching algorithm is used for CT-CBCT registration to correct a patient's setup because the alternative algorithm, intensity matching, takes a lot of time, approximately 10 - 20 minutes per patient. Thus our setup error data, which were retrospectively obtained, were provided by registration with the bone matching algorithm. This registration does not always give true setup error. Feature based registration algorithms, such as the bone matching algorithm is concerned about robustness. Our preliminary study found that the robustness of the bone matching algorithm was the same level as the intensity matching algorithm. In addition, we believe that 0.5 degrees, which is the maximum angular difference between an actual angle and a rounded angle, is too small to produce a large difference in a dose distribution. We were able to calculate the individual

dose distribution affected by setup errors of each case, and to assess the change of the dose distribution.

Conclusion

Dose distribution affected by actual setup errors of entire fractions were calculated for the three cases. We were able to assess the dose distributions of the plan with setup errors and found the following: the setup errors affected the dose around the beam edges, the DVHs, V95s and mean doses for the CTVs were mostly unchanged, and a part of the spinal cord of two of the cases had the dose changed by 5 – 10% due to setup errors.

References

1. AAPM, Dosimetric accuracy and equipment tolerances. In: AAPM Report 13 Physical aspects of quality assurance in radiation therapy. Huston Texas: AAPM; 1984. p. 7-13
2. Haslam JJ, Lujan AE, Mundt AJ, Bonta DV, Roeske JC. Setup errors in patients treated with intensity-modulated whole pelvic radiation therapy for gynecological malignancies. *Med Dosim.* 2003; 30: 36-42.
3. Dawson LA, Eccles C, Bissonnette JP, et al. Accuracy of daily image guidance for hypofractionated liver radiotherapy with active breathing control. *Int J Radiat Oncol Biol Phys*, 2005; 62(4): 1247-52
4. Kunzler T, Grezdo J, Bogner J, Birkfellner W, Georg D. Registration of DRRs and portal images for verification of stereotactic body radiotherapy: a feasibility study in lung cancer treatment. *Phys Med Biol.* 2007; 52: 2157-70.

5. Clippe S, Sarrut D, Malet C, Miguet S, Ginestet C, Carrie C. Patient setup error measurement using 3D intensity-based image registration techniques. *Int J Radiat Oncol Biol Phys.* 2003; 56: 259-65.
6. Jans HS, Syme AM, Rathee S, Fallone BG. 3D interfractional patient position verification using 2D-3D registration of orthogonal images. *Med Phys.* 2006; 33: 1420-39.
7. Munbodh R, Jaffray DA, Mosely DJ, Chen Z, Knisely JP, Cathier P, et al. Automated 2D-3D registration of a radiograph and a cone beam CT using line-segment enhancement. *Med Phys.* 2006; 33: 1398-411.
8. Munbodh R, Chen Z, Jaffray DA, Moseley DJ, Knisely JP, Duncan JS. A frequency-based approach to locate common structure for 2D-3D intensity-based registration of setup images in prostate radiotherapy. *Med Phys.* 2007; 34: 3005-17.
9. Létourneau D, Martinez AA, Lockman D, Yan D, Vargas C, Ivaldi G, et al. Assessment of residual error for online cone-beam CT--guided treatment of prostate cancer patients. *Int J Radiat Oncol Biol Phys,* 2005; 62: 1239-46.
10. Wang H, Shiu A, Wang C, et al. Dosimetric effect of translational and rotational errors for patients undergoing image-guided stereotactic body radiotherapy for spinal metastases. *Int J Radiat Oncol Biol Phys* 2008; 71(4): 1261-71
11. Hong TS, Tome WA, Chappell RJ, et al. The impact of daily setup variations on head-and-neck intensity-modulated radiation therapy. *Int J Radiat Oncol Biol Phys* 2005; 61(3): 779-88
12. Siebers JV, Keall PJ, Wu Q, Williamson JF, Schmidt-Ullrich RK. Effect of patient setup errors on simultaneously integrated boost head and neck IMRT treatment plans.

- International Journal of Radiation Oncology Biology and Physics 2003; 63: 422-33.
13. Lawson JD, Elder E, Fox T, et al. Quantification of dosimetric impact of implementation of on-board imaging (OBI) for IMRT treatment of head-and-neck malignancies. *Med Dosim* 2007; 32(4): 287-94
 14. Little DJ, Dong L, Levy LB, et al. Use of portal images and BAT ultrasonography to measure setup error and organ motion for prostate IMRT: implications for treatment margins. *Int J Radiat Oncol Biol Phys* 2003; 56(5): 1218-24
 15. Schaly B, Bauman GS, Song W, et al. Dosimetric impact of image-guided 3D conformal radiation therapy of prostate cancer. *Phys Med Biol* 2005; 50(13): 3083-101
 16. Yan D and Lockman D. Organ/Patient geometric variation in external beam radiotherapy and its effect. *Med Phys*. 2001; 28: 593-602
 17. van Herk M, Witte M, van der Geer J, Schneider C, Lebesque JV. Biologic and physical fractionation effects of random geometric errors. *Int J Radiat Oncol Biol Phys*, 2003; 57: 1460-71.

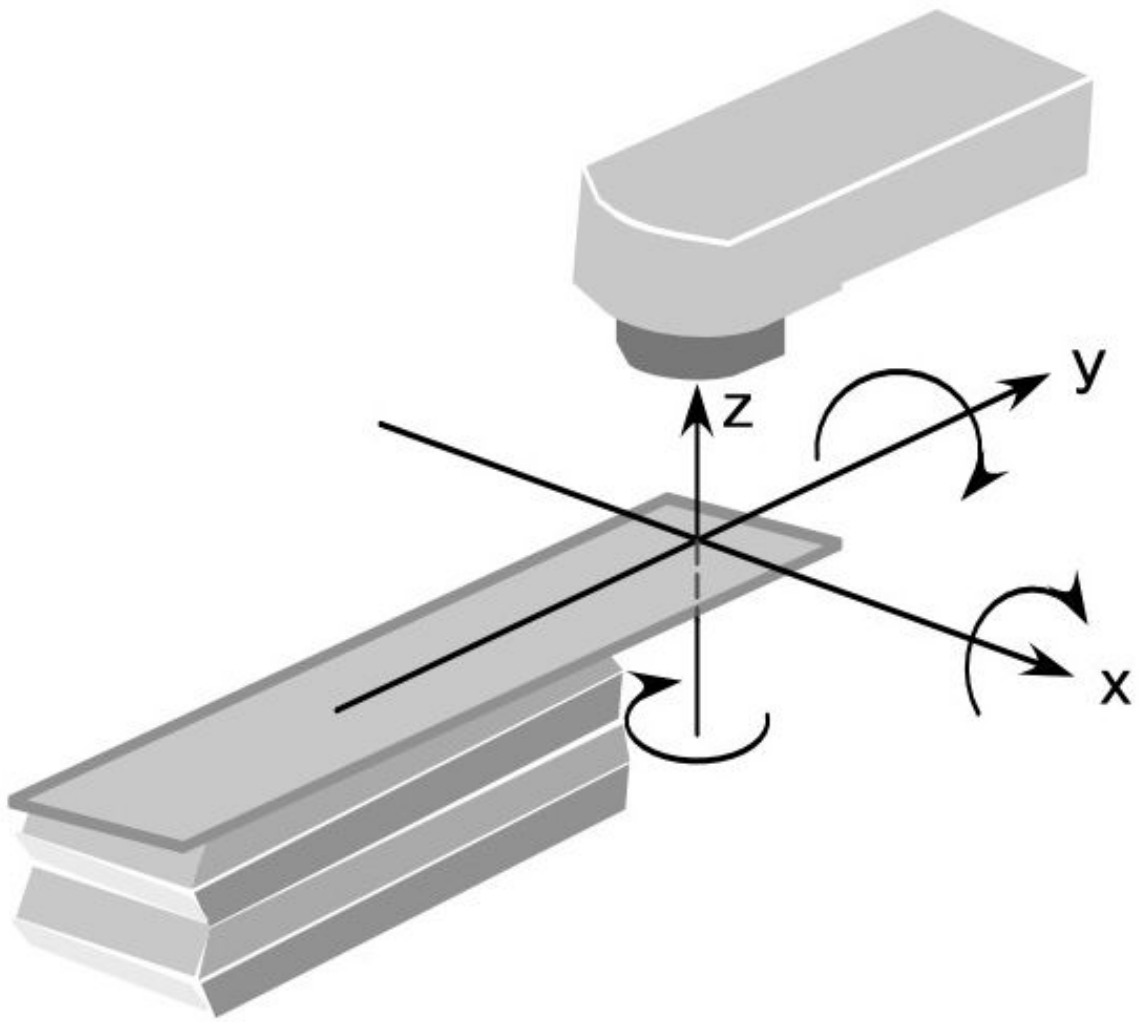


Fig 1 Coordinate system.

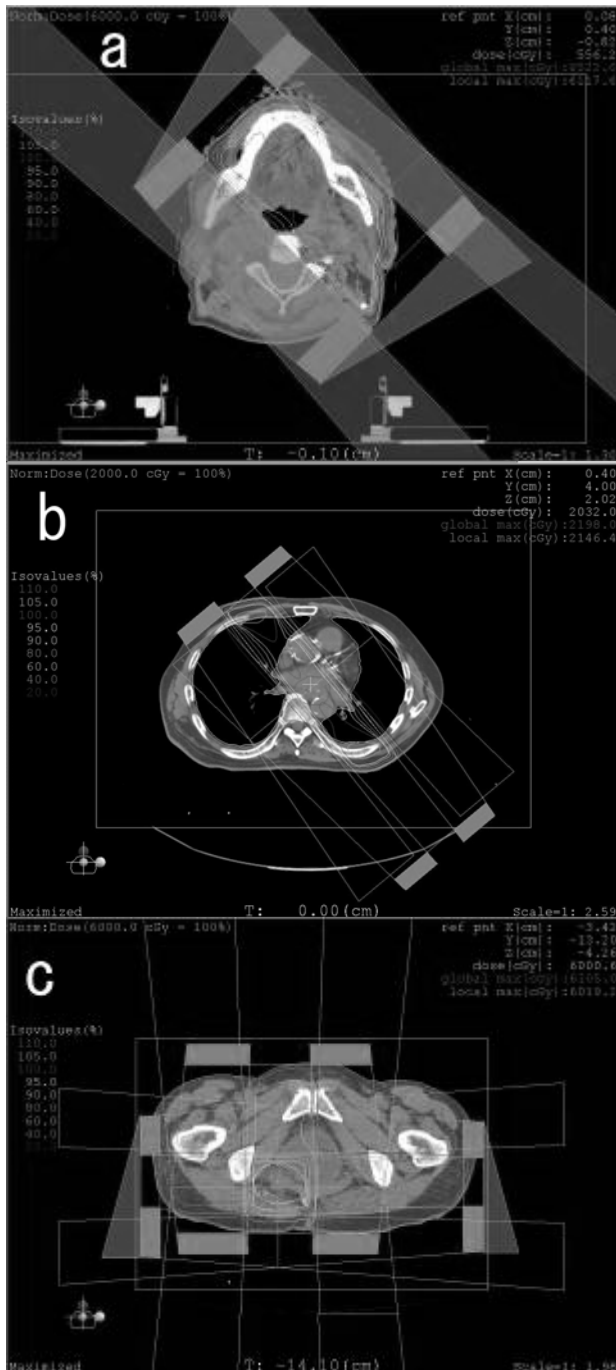


Fig. 2 The original approved plans.

Image a shows the radiotherapy plan for case A, image b shows case B, and image c shows case C.

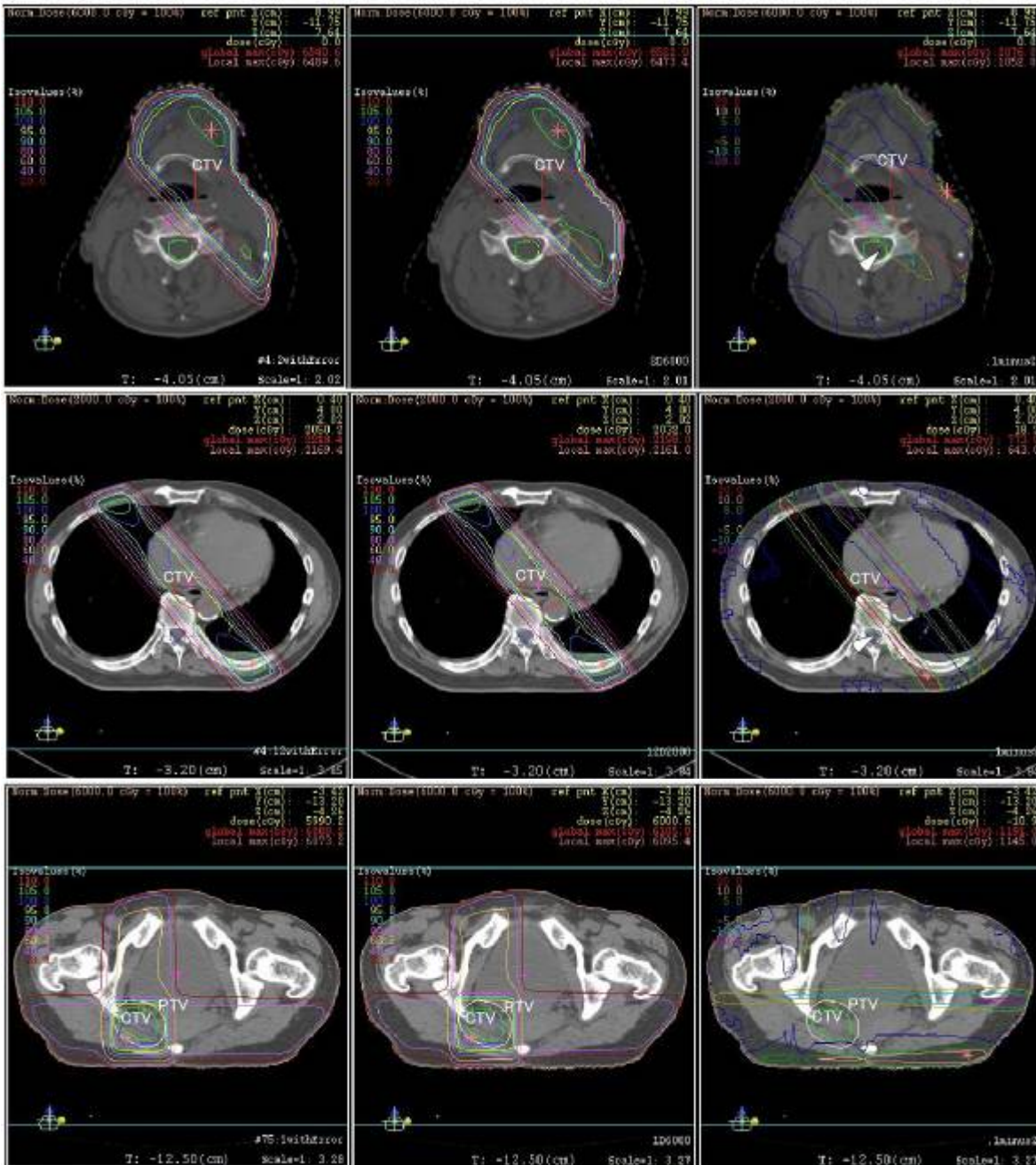


Fig 3 Dose distributions of the plans with setup errors and the original approved plans, and the differential dose distributions.

The top row shows the distributions for case A, the middle row shows the distributions for case B and the bottom row shows the distributions for case C. The left column shows the

dose distribution of the plan with setup errors, the middle column shows that of the original approved plan, and the right column shows the result of subtracting the dose distribution of the original plan from that of the plan with setup errors. The red lines in the images for cases A and B indicate the CTVs, and the green and white lines indicate the CTV and PTV for case C. The white triangles indicate a 5 or 10% different dose volume overlapped on the ORs.

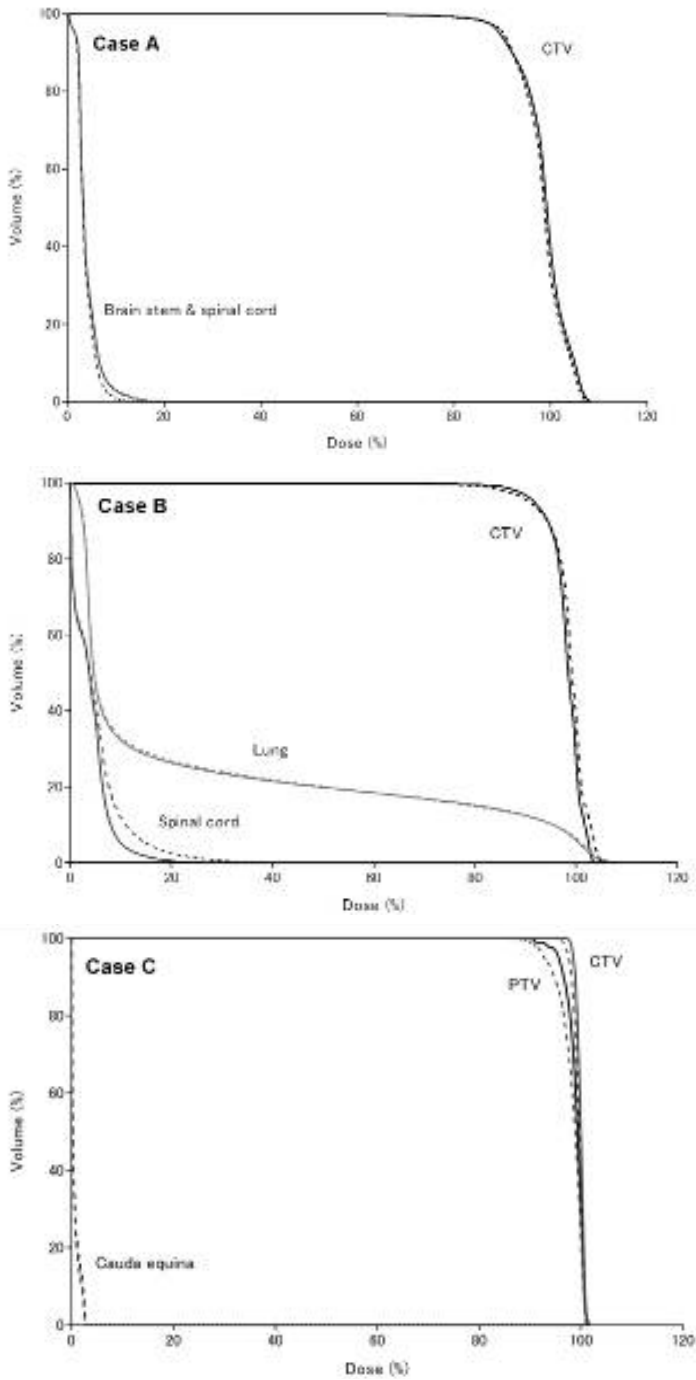


Fig. 4 Dose volume histograms.

The DVHs for cases A, B and C. Solid lines in all graphs illustrate DVHs in the original approved plan and dotted lines illustrate DVHs in the plan with setup errors.

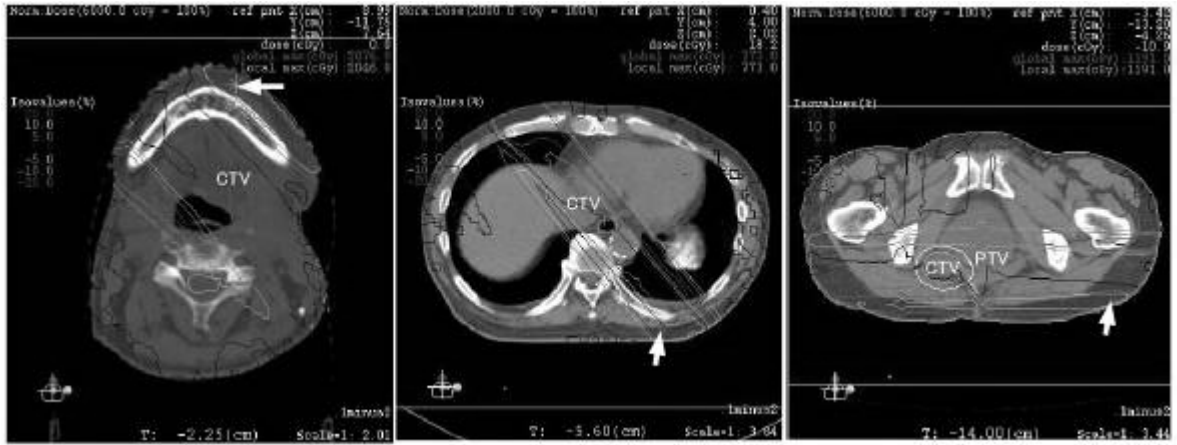


Fig. 5 The maximum dose difference point.

The arrows indicate the position where the dose was the most varied. The most varied doses occurred far from the isocenter and near the skin.

Table 1. Summary of cases and setup errors

Case	Age/ sex	Site	Primary	CTV (ml)	Energy (MV)	Beams/ fractions	Total dose (cGy)	Setup error (mean ± SD)	
								Translation (cm)	Rotation (deg)
A	62/M	neck	unknown, LN meta	256.2	6	2/30	6000	X 0.23±0.13	X -0.45±0.48
								Y -0.16±0.09	Y 2.06±1.21
								Z -0.01±0.13	Z 0.18±0.72
B	74/M	esophagus	esophagus Ca.	192.0	10	2/10	2000	X -0.05±0.25	X 2.32±0.92
								Y 0.02±0.23	Y 0.08±0.44
								Z -0.22±0.30	Z 0.53±0.96
C	50/F	coccygeal bone	rectum Ca. recurrence	24.1	10	4/20	6000	X 0.00±0.14	X -1.61±1.65
				(59.5)*				Y -0.19±0.29	Y 1.11±0.77
								Z -0.31±0.26	Z -0.91±0.43

*volume of planning target volume CTV: clinical target volume SD: standard deviation

Table 2. Results of dose distribution difference

Case	Maximum dose	Width of 10% iso-dose	V95 (%)		Mean dose (%)	
	difference (%)	volume in differential dose distribution (cm)	Approved plan	Plan with setup errors	Approved plan	Plan with setup errors
A	34.7	1.77	82.7	80.6	98.7	98.2
B	35.9	1.85	88.1	88.3	97.9	98.2
C	19.9	1.3	100 (96.8)*	99.9 (89.0)*	99.8 (98.9)*	99.4 (98.1)*

*Values in parentheses are for planning target volume